Novel Phased Array Laser Radar Architecture for Satellite Imaging and Identification

James R. Leger
Department of Electrical and Computer Engineering
University of Minnesota

Thang Hai Nam Au, Harsha Torke
Department of Electrical and Computer Engineering
University of Minnesota

ABSTRACT

We propose a radically new optical design that enables large angle laser beam steering, focusing, and beam forming over large optical apertures with a minimum of mechanical motion. Compared with conventional optical phased arrays, our design is capable of vastly larger steering angles, can address an order-of-magnitude larger number of object points, and is fully focusable, all accomplished by small displacements of light-weight fibers. Importantly, this imaging modality is capable of acquiring and tracking objects over substantial angles with no motion of large collimation optics. Second-order compensation of atmospheric turbulence can also be achieved with no additional hardware, resulting in improved beam quality on target.

Our architecture starts with a conventional coherent beam combining layout consisting of a single master oscillator laser driving an array of fiber amplifiers. Each fiber amplifier is collimated by a collimating optic to form a sub-aperture of the array. Active phase control establishes coherence across the array of sub-apertures, resulting in a large total diameter, low divergence beam at the transmitter and a high-resolution illumination beam at the target. A key innovation of our system consists of the micro-motion of the fiber amplifier delivery tip at each sub-aperture. Motion in the x- and y-directions produces an angular tip to the beam in each module. Motion in the z-direction provides a parabolic curvature. A coordinated motion of these three directions at each module can generate a large, steerable and focusable wavefront that extends across the entire array. The diameter of each sub-aperture can be modest in size making a large array of many coherently combined modules practical while still allowing beam steering over a substantial range and significant beam focusing.

A second innovation is to use the principle of diffractive optics to wrap the phase of the wavefront at the edge of each sub-aperture. Integer multiples of a wavelength are subtracted from the phase of each sub-aperture in such a manner that the phase at adjacent edges of two sub-apertures is identical (modulo 2π). If the linewidth of the laser is sufficiently narrow, this wrapped beam will perform identically to its continuous counterpart. Note that each sub-aperture assembly is highly modular, making the construction of large arrays considerably more practical.

Because the wavefront contained in each transmitting sub-aperture has a completely adjustable piston, tilt and misfocus component, any piecewise second-order wavefront can be established across the entire phased array. This flexibility in wavefront generation can be used to tailor the illumination beam to an arbitrary shape at the target. We use both iterative Fourier transform algorithms and genetic algorithms to solve for the phase distribution that produces the desirable beam shape at the target. Thus, along with a conventional raster scanning and imaging mode, our system is capable of identifying targets by comparing their reflected power to a dictionary of array-produced illumination shapes. This mode holds the promise of high-speed target detection combined with macro-motionless target tracking.

1. INTRODUCTION

Active imaging of satellites at GEO, x-GEO, and cislunar distances is challenging on many fronts. Conventional RF radar technology does not offer sufficient spatial resolution due to its large wavelength. Even at optical wavelengths, the required resolution and scanning/tracking performance stretches current technology to its limits, and many imaging scenarios are currently not practical. The required laser conditioning and scanning is conventionally achieved by mounting a collimated source on a steerable gimbal so that the center of the beam is pointed in the

desired direction. However, this results in a cumbersome and often expensive mechanical system with a large-angle scan speed that is limited by the mass of the optics. For scenarios that require large apertures such as GEO, x-GEO, and cislunar imaging, this approach rapidly becomes impractical.

A potential alternative configuration uses an array of coherent and phase-steerable optical sub-apertures to steer the beam. This phased-array technology replaces the large single aperture by many smaller ones (called sub-apertures in this paper) and achieves scanning with no mechanical motion by electronic phasing. This technology, including the required active phase control to compensate for atmospheric aberrations has been pioneered by the directed energy community. Unfortunately, while offering an effective solution for low-resolution RF systems, there are two inherent problems with using optical phased arrays for high resolution imaging. The first is that high resolution imaging requires a large array diameter, whereas large scanning angles require a small distance between sub-apertures. Thus, systems that require high resolution and large scanning angles require an impractical number of optical sub-apertures. For example, to image an object in a GEO orbit at 35,000 km with a Rayleigh resolution of 1 meter using light with a wavelength of one micrometer requires an array that is 35 meters in diameter. Conventional optical phased arrays, on the other hand, require a sub-aperture spacing that is smaller than approximately 60 micrometers to electronically scan a beam over one degree in angle, with larger scanning angles requiring even smaller spacing or complex mechanical scanning. Clearly, optical arrays do not offer a solution to a high-resolution system that is scannable over a large angular range with minimum mechanical motion. An additional problem with phased arrays is that the total number of resolvable points in an electronically scanned image can be shown to be approximately equal to the total number of sub-apertures in the array. Thus, for a high resolution, large area scan space, an impractically large number of sub-apertures is again required.

It is the aim of this paper to introduce a new laser scanning paradigm that combines a conventional phased array with micromotion, achieving significantly enhanced performance compared with traditional phased arrays. We start with a description of the array architecture and provide a paraxial analysis of scanning and focusing performance. Next, we compare the current optical configuration with known optical elements that are based on similar optical principles. The subsequent section describes a computer model that predicts the expected performance of a real system that is subject to aberrations and other real-world effects. We end with a study of the beam forming potential of an array that is produced by an arbitrary piece-wise second-order phase profile.

2. ARRAY ARCHITECTURE

The basic architecture described in this section was first introduced by us as a solution to the Breakthrough Starshot challenge [1] and has been reported in [2]. The following derivation follows this original derivation closely. The overall architecture, illustrated in fig. 1, shows the basic layout of the system. A single master oscillator fiber laser (MO, not shown) is split into several channels, where each channel consists of a phase modulator, a fiber amplifier, a true-time fiber delay line (TTD), and a collimating lens. Note that the lenses used in this diagram are for illustration purposes only and may be replaced by suitable mirrors or more complex optical systems.

The purpose of the phase modulator is to provide independent phase control over each channel, whereas the individual fiber delay lines are provided to keep the path lengths of each channel roughly equal. It is important to monitor the phase of each channel and adjust the phases of all the channels to be temporally stable and uniform. Assuming phase stability is achieved and the fill factor of the array is close to unity, this configuration optimizes the overall radiance of the system and maximizes the amount of energy that can be delivered to a distant target. This architecture is commonly used in coherent beam combining systems [3] for directed energy applications, where each individual fiber amplifier is capable of providing as much as one kilowatt of optical power to its respective channel [4].

The architecture shown in fig. 1 differs from a conventional coherent beam combining system by allowing the fiber tip of each channel to shift its 3D location by a small prescribed amount with respect to the focal point of its corresponding lens. The fiber output can be considered a point source by the lens, so placing the fiber tip at the focal point of the lens produces a collimated beam directed normal to the lens. However, small changes in the fiber tip location will result in linear phase shifts (by moving the fiber in a transverse direction) or a quadratic phase shift (by moving the fiber longitudinally with respect to the lens). Through a coordinated set of fiber tip motions across the array, a general piece-wise second-order phase function can be established across the array, greatly increasing the

functionality of the system. In the following sections of this paper, we will show how wide-angle beam scanning, beam focusing and generalized beam forming can all be achieved with these fiber micro-motions.

To understand how our proposed array architecture can create an arbitrary piece-wise second-order phase distribution, we consider the case of an output beam that requires a specific tilt angle (i.e. a linear phase shift) and a specific amount of focal power (i.e. quadratic curvature) to illuminate a unique point in 3D space. This is illustrated in fig. 2a, where

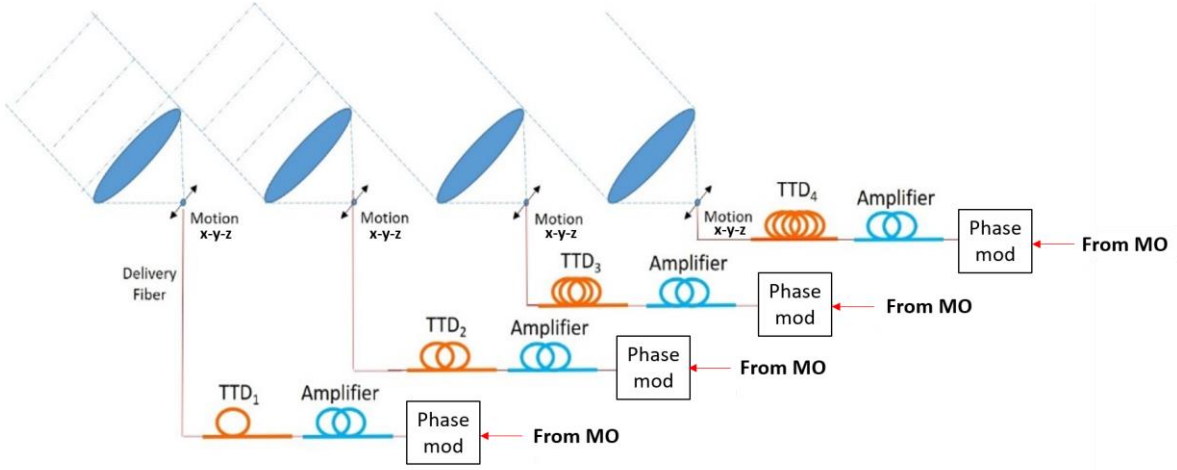

Fig. 1. Phased array architecture. Figure adapted from [2].

the linear and quadratic components are shown separately (dashed black and solid green curves) and also combined (solid red curve). We consider the case where each sub-aperture of the array must reproduce a portion of the tilted parabolic phase distribution shown in the figure. The overall required phase $\phi(x, y)$ across the entire output aperture is given by eq. 1:

$$\phi(x,y) = k\left[\gamma_x x + \gamma_y y - \frac{x^2+y^2}{2z_0}\right], \quad (1)$$

where γ_x and γ_y are the direction cosines in the x- and y-directions with respect to the center of the array, z_0 is the location of the spherical wave focus in the z-direction generated by the array, and $k = 2\pi/\lambda$ is the wavenumber of

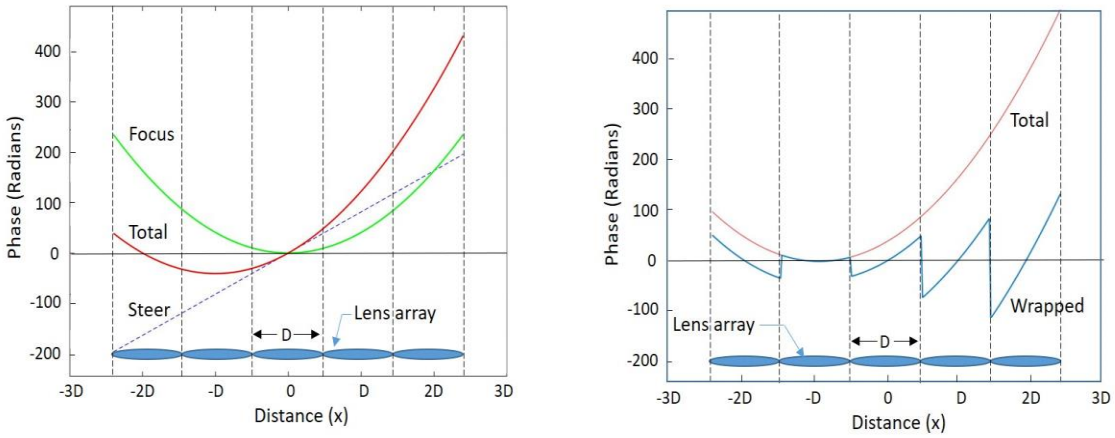

(a) (b)

Fig. 2. *a) Required phase distribution to achieve beam scanning and beam focusing. Note that the focus term is shown as a positive quadratic function for clarity. b) Wrapped phase distribution formed by subtracting integer numbers of wavelength at the edge of each sub-aperture. Figure adapted from [2].*

the light with a wavelength λ. The sign of the quadratic term is chosen to be negative, corresponding to a converging beam.

To understand the required individual phase shapes at each laser sub-aperture, it is useful to write the phase in eq. 1 as a Taylor expansion, where the expansion is performed around the center of each sub-aperture lens. We assume that the lenses are close-packed such that their diameters and spacing are both D. The Taylor expansion is performed at points $x = x' + mD$ and $y = y' + nD$, where m and n are integers corresponding to the specific sub-apertures. The expansion can then be written as:

$$\phi(x,y)|_{\substack{x=mD+x' \\ y=nD+y'}} = \frac{2\pi}{\lambda}\left[\gamma_x mD - \frac{m^2D^2}{2z_0} + \gamma_y nD - \frac{n^2D^2}{2z_0}\right] + \frac{2\pi}{\lambda}\left[\gamma_x - \frac{mD}{z_0}\right]x' + \frac{2\pi}{\lambda}\left[\gamma_y - \frac{nD}{z_0}\right]y' - \frac{\pi}{\lambda z_0}[x'^2 + y'^2] \quad (2)$$

where x' and y' are referenced to the center of the lens corresponding to the (m,n)th sub-aperture. The first term in brackets represents a constant (or piston) phase. The second and third terms in brackets correspond to linear phase changes (or phase tilts) in x' and y' respectively. Finally, the last term in brackets shows the required quadratic phase curvature (or focus). We now show that these wavefronts can be generated at the (m,n)th sub-aperture by simple displacements of the fiber tip in the transverse and longitudinal directions.

Fig. 3 shows a more detailed diagram of the optics corresponding to a single channel, where the optical axis has been drawn to correspond to the vertical axis.

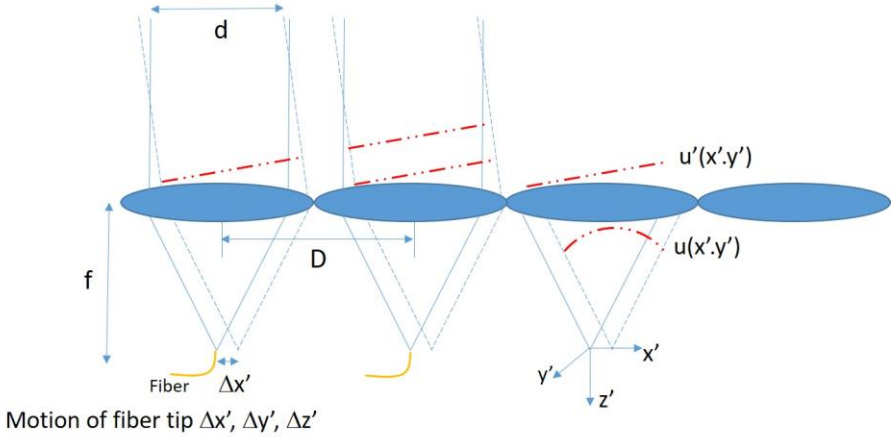

Fig. 3. Details of the collimation optics. Figure adapted from [2].

We assume that the fiber tip is displaced in the x', y', and z' directions by the values Δx', Δy' and Δz' respectively from the lens focal point. The wavefront that is incident on the lens is then given by

$$u(x',y') = \exp\left[i\,\pi\,\frac{(x'-\Delta x')^2+(y'-\Delta y')^2}{\lambda(f+\Delta z')}\right], \quad (3)$$

where we recall that the (x',y') coordinates are centered at the optical axis of each lens. The wavefront that exits the lens is given by multiplying eq. (3) with the transmittance of the lens. The resulting wavefront contains three terms:

$$\phi_1(x',y') = \frac{\pi(\Delta x'^2+\Delta y'^2)}{\lambda(f+\Delta z')} \text{ (Piston)} \quad (4)$$

$$\phi_2(x',y') = -\frac{2\pi(\Delta x'\,x' + \Delta y'\,y')}{\lambda(f+\Delta z')} \text{ (Tilt)} \quad (5)$$

$$\phi_3(x',y') = -\frac{\pi\,\Delta z'\,(x'^2+y'^2)}{\lambda f(f+\Delta z')} \text{ (Quadratic)} \quad (6)$$

It is clear that these three fiber motions are sufficient to reproduce the phases required in eq. (2). In particular, by equating terms we find the following requirements on fiber motion for small values of Δz' with respect to f:

$$\Delta x' \cong -f\left[\gamma_x - \frac{mD}{z_0}\right],\ \Delta y' \cong -f\left[\gamma_y - \frac{nD}{z_0}\right],\ \Delta z' \cong \frac{f^2}{z_0} \tag{7}$$

where the requirement that $\Delta z' \ll f$ is equivalent to $z_0 \gg f$, which is the case for satellite imaging. We note that eq. (2) seems to require a potentially large piston change as well given by the first term in brackets. However, since a phase function repeats itself every 2π radians, rather than use this large phase value we can instead use a modulo 2π version of it. The removal of integer multiples of a wavelength allows the piston phase term to be restricted to a range between 0 and 2π radians, making it easy to generate by a simple phase modulator (for example, by using the phase modulators in fig. 1 or by using sub-wavelength motion of the fiber in the z-direction). This discontinuous phase function, shown in fig. 2(b), behaves exactly like its continuous counterpart for sufficiently narrow-band light. In essence, the phase fronts at the edges of two channels are adjusted so that there is no phase discontinuity except for multiples of 2π radians. We note, however, that the phase delays are no longer "true time" and so there is a condition placed on the coherence length of the laser and hence its bandwidth.

The actual piston phase of each channel is not only governed by the location of the fiber tip, but is influenced by random changes in the fiber temperature and other environmental effects. Thus, in a practical system a feedback loop would have to be used to ensure the proper phase state is maintained.

3. COMPARISONS WITH ALTERNATIVE OPTICAL SCANNING ARCHITECTURES

The architecture of a traditional phased array is similar to that shown in fig. 1. However, the fibers are fixed at the focal points of the lenses and only the piston phase of each channel can be adjusted (usually by an electrooptic phase modulator). This places a severe restriction on its maximum scan angle. As described in the introduction, the maximum scan angle that can be achieved by a traditional phased array is given by $sin(\theta) = \pm \lambda/2D$, where θ is the scan angle, *D* is the spacing between sub-apertures, and λ is the wavelength of light. Significant scan angles can only be achieved if *D* is small, making this scanning method impractical for large diameter arrays. Viewed as a diffraction grating, a traditional phased array can be viewed as a grating where only the first order diffraction term is accessible. On the other hand, our architecture allows one to blaze the grating to high orders simply by placing a phase tilt across each of the sub-apertures. Since the scan angle is proportional to the blaze number, these high-order gratings have intrinsically larger scan angles. And since the "blaze" of the laser array is adjustable by moving the fibers in the x and y directions, access to a complete set of higher diffraction orders increases the accessible range of the array significantly.

A second property illustrated by the grating picture is apparent in the number of discrete scan angles that can be uniquely addressed by the scanner (sometimes called the space-bandwidth product of the grating). In a traditional grating, this number is given by the number of grating lines (or sub-apertures in the case of the laser array) multiplied by the grating order. Gratings that are blazed to work at higher grating orders have intrinsically larger space-bandwidth products. Thus, our proposed array typically has a space-bandwidth product that is significantly larger than a simple phased array.

It is also instructive to compare the present system with a beam steering method that uses two microlens arrays [5]. This configuration is shown in fig. 4(a), consisting of a two-dimensional array of lenses (shown in one dimension for simplicity). Beam steering is accomplished by shifting one lens array with respect to the other. It is clear from the picture that a shift of focused spots caused by translating the first lens array will cause the collimated beams exiting the second array to be tilted. However, because the phase jumps between the outputs of adjacent lenses are not always an integer multiple of 2π, there are only specific angles that are accessible by this device, as shown in fig. 4(b). The allowed scan angles are shown in red, and the amount of light in each scan angle is indicated by the dashed line. It is clear that a translation of the first lens array by an amount Δx shifts the dotted line over the allowed scan angles by an amount $\Delta x/f$. At particular amounts of shift Δx, a scan angle can contain 100 % of the light. However, at other amounts of shift, the light is spread out among many allowed angles. More importantly, it is impossible with this system to address light between these allowed angles.

The present scanning system can be viewed as a modification of this lens array scanning method by replacing the first lens array with a set of fibers, as shown in fig. 5(a). If we imagine the simplest case of translating all the fibers together, this arrangement is identical to using the pair of lens arrays shown in fig. 4. However, there is an additional degree of freedom in the system shown in fig. 5 given by the phase adjustment in each fiber. As seen in fig. 5(b), the fiber motion Δx shifts the dashed line as before. However, by adjusting the phase of each fiber to establish a linear phase shift across the array, the allowable scan angles can be made to shift as well so that one of them is always centered at the peak of the dashed curve. The degree of phase shift is given by the piston term in eq. (2). Thus, all angles can be addressed with 100 % efficiency and there are no gaps in allowable scanning angles.

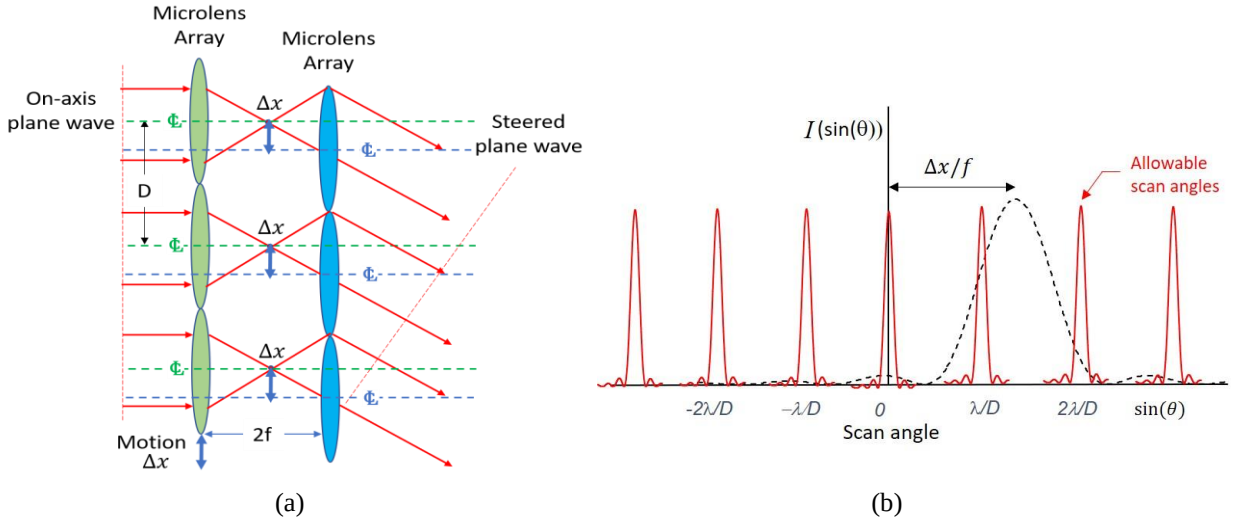

Fig. 4. Microlens array beam steering. a) Effect of shifting the first microlens array. b) The allowed steering angles are fixed to the positions shown in red and their relative efficiencies vary as the dotted curve moves with array translation.

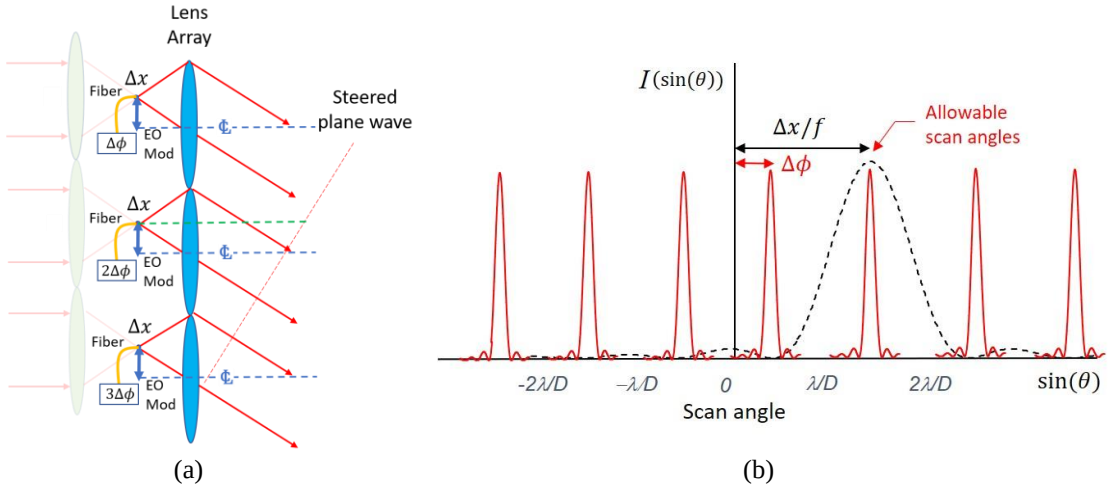

Fig. 5. Analogy between the proposed laser scanning system and scanning with microlens arrays. a) The first lens array is replaced by fiber tips, the fiber outputs are all moved together by an amount Δx, and the phases of the fiber outputs are modified electronically. b) The allowed steering angles, shown in red, can be shifted by changing the phase of the fibers in a linear fashion. All scan angles can be addressed with an operating efficiency of 100 %.

4. ESTIMATION OF ARRAY PERFORMANCE

There are several practical issues that limit the performance of our laser array. A reduced fill factor resulting from gaps between sub-apertures will reduce the Strehl ratio by generating grating lobes that rob the central lobe of

power. Lens aberrations can distort each beam exiting a sub-aperture, reducing the power at the target and compromising the resolution of the system. Translating the fiber without an accompanying fiber angle correction can cause the light to partially miss its corresponding objective lens, again resulting in reduced power. We have modeled many of these effects in an attempt to study the limits of our beam forming architecture.

The basic model consists of a ray trace analysis of the approximately Gaussian beam that exits the fiber. The rays are traced through lenses obtained from a commercial lens catalog and an aberration profile of the exiting beam is calculated for each lens. Ray traces are calculated using Snell's law using the refractive index values taken from the glass manufacturer datasheet at an optical wavelength of 1060 nm.

The light from the array is propagated to the far field using traditional Fourier optics approaches. The Strehl ratio is then calculated by comparing the power at the center of the scanned and focused spot with the theoretical power that could be obtained from a system with no aberrations or other deficiencies. The system under test is a hexagonally closed-packed array with Gaussian illumination. Gaussian illumination was modeled with a variety of Gaussian widths. The optimum Gaussian width produced a Strehl value of 0.8145 for a single sub-aperture, in agreement with analytical predictions. This is the profile used for all simulations.

Fig. 6 shows a graph of the Strehl ratio as a function of the f/# of the collimating lenses and the scan angle. The lens design was optimized by starting with a catalog lens and modifying its prescription to obtain the best Strehl ratio over a specified scan angle. Lenses under consideration were derived from Thorlabs C coated lenses analyzed at a wavelength of 1060 nm. Prior to simulation, target lenses were optimized in Zemax OpticStudio using field angles ranging up to 15 degrees off axis in both x and y directions. After optimizing the lens geometry for steering angle, a second re-optimization was applied to ensure the focal distance of the new lens matches the intended f/#.

The optimized solution had excellent performance over large scan ranges for all but the lowest f/# modeled. The fall-off with angle is mainly a result of off-axis aberrations from the lens, many of which are exacerbated at lower f/#s. Low f/# lenses having reduced performance is a well-documented phenomenon in line with expectations. While increasing f/# tends to reduce the effect of aberrations, the fiber displacement required for a given steering angle also increases, which may be constrained by mechanical limitations.

A parameter sweep of target focal distance shows that while high f/# lenses show better performance at large beam steering angles, lower f/# lenses actually show better performance when targeting shorter propagation distances. This is because the lower f/# lenses require shorter fiber displacements and incur diminished aberrations compared to higher f/#. For cases where focusing is required to a short target distance, a significant field curvature is required across the aperture. This means that sub-apertures at the edge of the array require a significant fiber displacement, which is exacerbated using high f/# lenses.

In addition to comparing differing f/#s, a variety of lens diameter and lens geometry were explored. Simulations show that an array composed of smaller sub-apertures results in higher performance, owing to the increasing aberrations as lens diameter increases. For the Thorlabs lenses considered, it was also noted that less complex geometries allow for wider steering range, with singlet lenses producing better results than doublet lenses. For this observation it should be noted that the selected lenses were not intended for wide angle beam steering, even after re-optimization. Therefore, custom designed beam steering lenses may still offer better performance.

5. BEAM FORMING

One of the most intriguing aspect of our optical phased array is the ability to generate arbitrary piece-wise second-order phase functions. By choosing the appropriate phase distribution, it is possible to modify the beam shape and other beam characteristics.

Vortex beam generation. Fig. 7(a) shows a laser array consisting of hexagonal close-packed circular apertures that contain a spiral phase pattern designed to produce a vortex beam. Fig. 7(b) shows the far-field pattern generated by the vortex beam, exhibiting the expected donut shape in the center of the diffraction pattern.

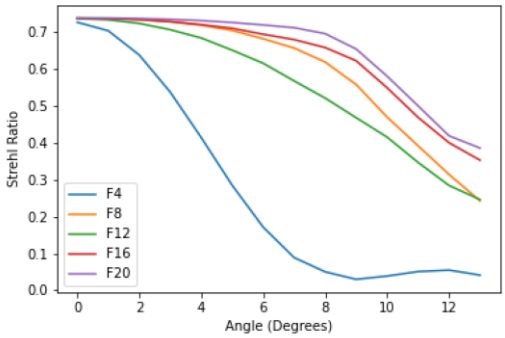

Fig. 6. Strehl ratio as a function of scan angle for an optimized lens array.

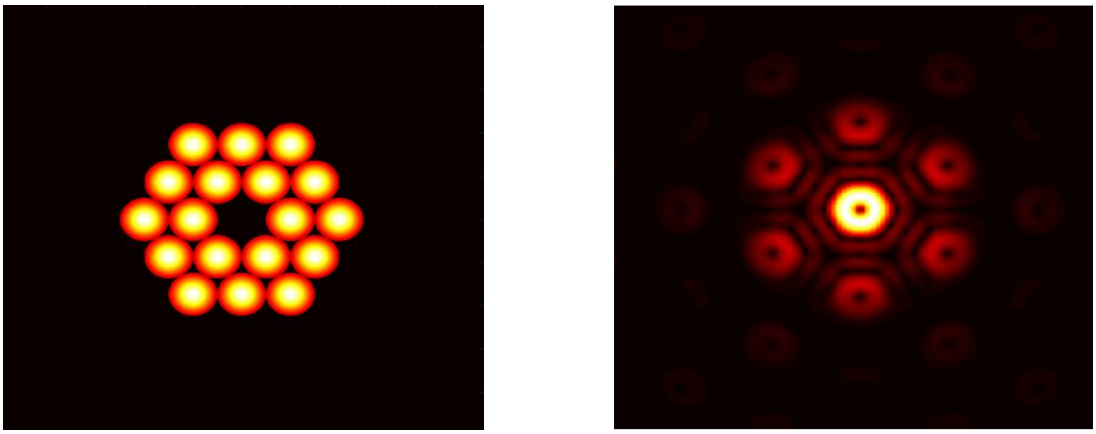

(a) (b)

Fig. 7. Generation of an optical vortex beam. a) Transmitter array. b) Far-field diffraction pattern.

A vortex beam topology is produced by optimizing the field distribution to minimize error when compared against a phase profile defined by $exp[i\ 2\pi\ N\ tan^{-1}(y/x)]$, where N is the desired vortex order. In a phased array system this is accomplished by applying a phase shift to each fiber based on its position in the array, and applying an x- and y-shift to the fiber to produce a phase gradient across the sub-aperture. The current architecture does not include a mechanism to apply a circular phase pattern across a single sub-aperture. As such, the center lens is left dark or removed from the array.

Far-field image generation. One possible satellite detection scheme generates light patterns that match the shape of a particular satellite and measures the integrated return. In this method, a dictionary of satellite shapes is generated and applied sequentially to the object. Beam forming can be achieved using a conventional laser phased array by choosing the proper phase distribution at the array to produce a given far-field pattern. For arrays that contain a large number of sub-apertures, the space-bandwidth product of the array is sufficiently high to achieve reasonable results using standard diffractive optics design methods. For instance, we have used the Gerchberg-Saxton phase retrieval algorithm [6] to synthesize an intensity distribution at the satellite by a proper selection of the phases, one for each sub-aperture. However, for more practical array sizes containing a modest number of sub-apertures, new methods must be employed.

A significant improvement can be achieved using the fiber-shifting phased array of this paper. Rather than restricting each sub-aperture to a single piston phase value, the sub-aperture can now contain a more complex

distribution described by an arbitrary piece-wise second-order function. The optimization problem now consists of adjusting four components per sub-aperture: piston phase, x-tilt, y-tilt, and quadratic curvature. These quadratic functions can change from sub-aperture to sub-aperture and the resulting imagery is no longer limited to the space-bandwidth product restrictions of a traditional phased array. Fig. 8 is a dramatic illustration of this advantage. Fig. 8(a) shows the desired reconstruction consisting of a simple block model of a satellite that is approximately the size of the Hubble space telescope (14 meters in length). The transmitter array was chosen to consist of a 5x5 array of rectangularly close-packed square apertures, each with an aperture size of 3 meters. A genetic optimization algorithm (GA) [7] was used to adjust the sub-aperture parameters. In fig. 8(b), the GA was used to select a simple constant phase for each aperture, similar to a traditional optical phased array. It is clear that the array is not able to reconstruct the satellite target image with high fidelity. In fig. 8(c), the GA was extended to adjust the overall phase as well as the tip-tilt parameters of the transmitter array achieved by fiber motion in the x-y direction. The result is a far more accurate reconstruction of the image. Fig. 8(d) shows the resulting phase distribution that is required at the transmitter. Note that the array consists of only 5x5 sub-elements, but that each element can contain both a constant (piston) and linear (tip-tilt) phase term.

Several items are worth noting in these simulations. First, we have restricted the array to only contain constant and linear phase terms. The addition of a quadratic term has the potential to further improve the imaging performance. Second, whereas the ultimate resolution of the array is not improved by including linear and quadratic phase terms, the space-bandwidth product of the array is dramatically increased. This means that much larger satellite images can be reproduced with the same 5x5 array, containing many more resolvable points. The degree of enhancement is governed by the limits on fiber motion (which controls the amount of tip-tilt and misfocus). These limits are ultimately determined by the collimating optics aberrations.

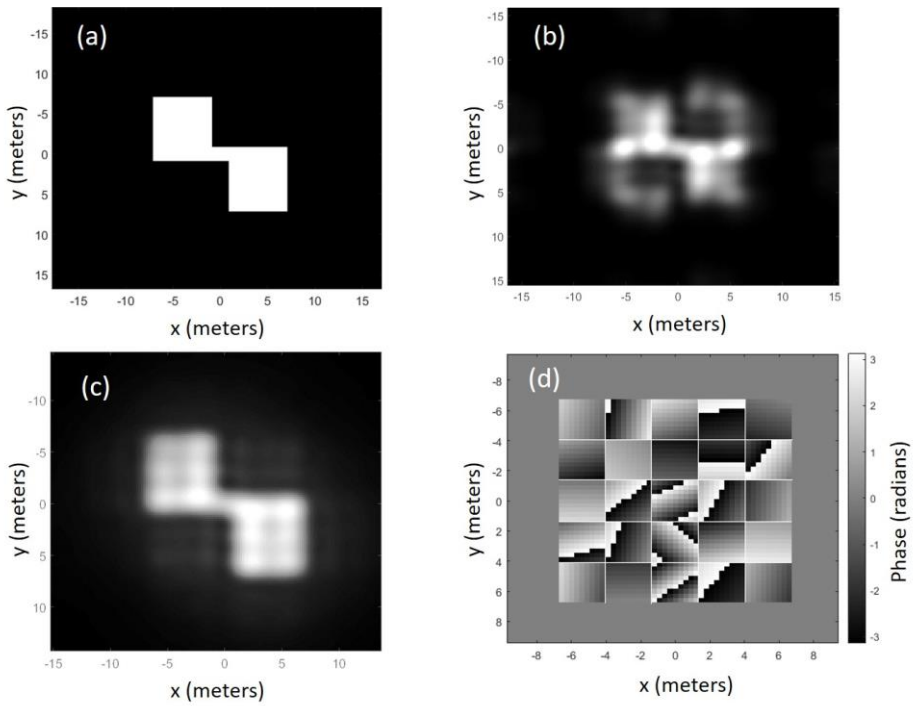

Fig. 8. Image formation in the far-field using piston and linear phase functions. The transmitter array consisted of a 5x5 array of close-packed square apertures, each aperture with a size of 3x3 meters. The propagation distance was chosen to be 35,000 km (approximately geosynchronous orbit) and the image size was chosen to be 14 meters in total length (approximately the size of the Hubble space telescope). The speckle contained in each image was removed by averaging across many realizations of the image. a) A representation of the desired image. b) The resulting far-field image using piston-only phases. c) The resulting far-field image using both piston and tip-tilt phases. d) A phase map of the 5x5 sub-apertures producing the image in (c).

6. CONCLUSIONS

We have introduced a novel architecture for laser beam steering that is capable of large angle scanning, focusing and beam forming with only small motions of the array fiber feeds. A physical model of the resulting beam indicates that the array can be scanned and focused over a substantial distance compared with a traditional phased array before optical aberrations limit its performance. The beam shaping ability of the array was also simulated using a genetic algorithm for phase optimization. Modeling results indicate that using a combination of both piston and tip-tilt adjustments of the individual sub-apertures can significantly improve the beam shaping ability of the array when compared with a traditional optical phased array.

7. ACKNOWLEDGEMENTS AND DISCLOSURES

The research reported here is supported by a subaward of AFOSR grant no. FA9550-23-1-0536. The basic architecture described in this paper was previously reported in the SPIE Optics and Photonics conference (2020) and the derivation of the theoretical underpinnings largely follow the presentation in [2]. All other parts of this paper represent original contributions.

8. REFERENCES

[1] Philip Lubin, "A Roadmap to Interstellar Flight", *Journal of the British Interplanetary Society* **69** (2016).
[2] James R. Leger, "A novel design for beamforming the Breakthrough Starshot laser array," *Proc. SPIE 11486, Laser Beam Shaping XX*, 114860D, https://doi.org/10.1117/12.2569134 (20 August 2020).
[3] A. Shirakawa, T. Saitou, T. Sekiguchi and K. Ueda: "Coherent addition of fiber lasers by use of a fiber coupler," *Optics Express* **10**, 1167–1172 (2002).
[4] M. N. Zervas and C. A. Codemard, "High Power Fiber Lasers: A Review," *IEEE Journal of Selected Topics in Quantum Electronics* **20**, 219-241 (2014).
[5] W. Goltsos and M. Holz, "Agile beam steering using binary optics microlens arrays," *Opt. Eng.* **29**, 1392–1397 (1990).
[6] R. W. Gerchberg and W.O. Saxton, "A practical algorithm for the determination of the phase from image and diffraction plane pictures", *Optik* **35**, 237–246 (1972).
[7] Jianyu Ye, XiaoCong Yuan, and Guangya Zhou, "Genetic algorithm for optimization design of diffractive optical elements in laser beam shaping," *Proceedings of the SPIE*, **V. 4594**, 118-127 (2001).